DOI: 10.1002/ejic.200600879

(Indenyl)ruthenium Complexes Containing 1,1′-Bis(diphenylphosphanyl)-ferrocene (dppf) and Thiolato Ligands: Synthesis, X-ray Structure Analysis, Electrochemistry and Magnetic Studies

Sin Yee Ng,[a] Weng Kee Leong,*[a] Lai Yoong Goh,*[a] and Richard D. Webster[b]

Keywords: (Indenyl)ruthenium / Thiolates / dppf / Cyclic voltammetry / ESR / Ruthenium

The reaction of [(Ind)Ru(dppf)Cl] (Ind = η^5-C_9H_7) (**2**) with RSNa {R = Me, Et, Ph, $Ph_2P(CH_2)_2$} proceeds in MeOH to give [(Ind)Ru(dppf)(SR)] {R = Me (**3**), Et (**4**), Ph (**5**), $Ph_2P(CH_2)_2$ (**7**)}, as well as [(Ind)Ru(dppf)H] (**6**), in all cases except for R = Ph. This R-dependence of the product mixture was rationalised on a RS^-/MeOH ↔ MeO^-/RSH equilibrium involving the interaction of thiolate (RS^-) with MeOH, and the relative nucleophilicities of RS^- versus MeO^-; **6** arose from β-H elimination from an OMe derivative. Cyclic voltammetric measurements on **2**, **3**, **4** and **5**, as well as the Cp (η^5-C_5H_5) and Cp* (η^5-C_5Me_5) analogues of **2**, indicated that the formal oxidation potentials for [LRu(dppf)Cl] complexes {L = Ind (**2**), Cp (**2A**) and Cp* (**2B**)} occurred in the order Cp* < Ind < Cp, correlating with the more electron-donating groups lowering the oxidation potentials. EPR experiments performed on the one-electron oxidised forms of **3** and **5** indicated paramagnetic compounds with *g* values close to 2, while the two-electron oxidised forms of **3** and **5** were diamagnetic. All the complexes were characterised spectroscopically, and **5** and **6** also crystallographically.

Introduction

The development of the chemistry of indenyl complexes of ruthenium(II) could be considered to date from the high-yield synthesis of [(Ind)Ru(PPh_3)$_2$Cl] (Ind = η^5-C_9H_7) (**1**),[1] which superseded [(Ind)Ru(CO)$_2$]$_2$, a low-yield compound,[2] as the common source material for the synthesis of (indenyl)ruthenium complexes. A recently improved synthesis of [(Ind)Ru(COD)Cl][3] has provided yet another alternative starting material. The initial interest in the indenyl ligand stems from its resemblance to η^5-cyclopentadienyl Cp/Cp* ligands, the 'pillar' ligands of transition-metal organometallic chemistry; subsequent interest was heightened by the observation of the so-called indenyl effect, an enhancement of reactivity of the complex brought about by facile ring slippage from η^5 to η^3 involving aromatisation of the benzene ring.[4]

In the last decade Gimeno's group have carried out intensive studies, with emphasis on reactivity, including catalytic aspects, particularly of vinylidene and allenylidene derivatives of ruthenium half-sandwich complexes.[5] Prior to these, there had been limited reports from various groups on studies of indenyl complexes of Fe, followed by those of the Group 6, 7 and 9 metals.[6] Recently reports of a few (indenyl)Ru complexes carrying N-containing ligands have emerged,[7] but to date there is only one report of examples carrying S-donor ligands, viz. EtS and EtMeS.[8]

In recent work, we have performed a comparative study of the reactivity of [(η^6-C_6Me_6)Ru(dppf)Cl] and [CpRu(dppf)Cl] (**2A**) with various nucleophiles, including S donor ligands.[9] It is therefore of interest to include the indenyl analogue of these in the comparison. This paper describes the reactions of [(Ind)Ru(dppf)Cl] (**2**) with simple alkyl/aryl monothiolates, RS^- (R = Me, Et and Ph), to compare with reported analogous reactions of [(Ind)Ru(PPh_3)$_2$-Cl] (**1**) with EtSNa,[8] and the comparative electrochemistry studies of [LRu(dppf)Cl] {L = Ind (**2**), Cp (**2A**) and Cp* (**2B**)} and [LRu(L′$_2$)Cl] (L = Ind, Cp and Cp*; L′$_2$ = dppm, dppe and dppf).

Results and Discussion

[(Ind)Ru(dppf)Cl] (**2**) was synthesised from phosphane substitution of [(Ind)Ru(PPh_3)$_2$Cl] (**1**), following a published procedure for the Cp analogue.[1]

Chloro Substitution

(a) Reaction of 2 with RSNa [R = Me (3), Et (4), Ph (5)] and Solvent Dependence

The reaction of **2** with an excess of RSNa in alcoholic solvent (MeOH or EtOH) at room temperature gave

[a] Department of Chemistry, National University of Singapore, 3 Science Drive, Singapore 117543
Fax: +65-6779-1691
E-mail: chmgohly@nus.edu.sg
chmlwk@nus.edu.sg
[b] Division of Chemistry and Biological Chemistry, Nanyang Technological University, Singapore 637616

[(Ind)Ru(dppf)(SR)] in R-dependent yields. (NOTE: with 1 equiv. of RSNa, the reaction at r.t. did not reach completion even after 18 h.) In the cases of R = Me and Et, a hydride complex, [(Ind)Ru(dppf)H] (**6**), was also isolated in about 20% yield (Scheme 1).

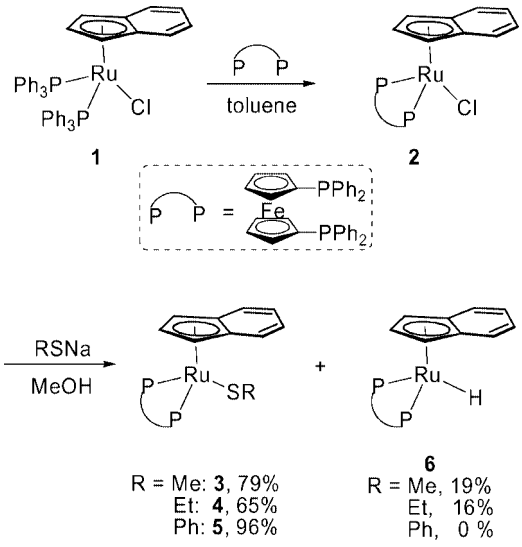

Scheme 1.

The latter complex was not anticipated, as hydride formation was not reported in the preparation of [(Ind)-$Ru(PPh_3)_2(SEt)$] from the reaction in refluxing THF of [(Ind)$Ru(PPh_3)_2Cl$] (**1**) with NaSEt,[8] or in similar syntheses of [$CpRu(PPh_3)_2(SR)$] (R = 1-C_3H_7, $CHMe_2$ and 4-C_6H_4Me).[10] Very recently, Gimeno and co-workers obtained mono- and diphosphane analogues of **6** from the reaction of [(Ind)Ru(P-P)Cl] {P-P = diphosphanes (dppm, dppe) or bis(PR_3)} with an excess of MeONa in MeOH.[11] The formation of metal hydrides from alkoxide precursors by β-hydrogen elimination is a well-established phenomenon.[12,13] Invoking the role of alkoxide in this reaction involving the use of thiolates in MeOH will require the participation of an equilibrium represented by Equation (1).

$$RS^- + MeOH \overset{K}{\rightleftharpoons} MeO^- + RSH \quad (1)$$

In such a situation the competition of nucleophiles RS^- and MeO^- in displacement of X from [(Ind)Ru(dppf)X] (X = Cl or MeOH) comes into play. This will depend on their relative nucleophilicities ($RS^- > MeO^-$), as well as the preponderance of one species over the other, a direct consequence of the equilibrium constant *K*. This is in agreement with the order of pK_a's in MeOH of the thiols as follows: MeSH (14.3)[14] ≤ EtSH (14.4)[15] > PhSH (10.9).[16] Thus, under similar concentrations of reactants, [MeO^-] in equilibrium (2) from PhS^- will be about two orders of magnitude lower than that from RS^- (S = Me or Et). This is in agreement with the observed absence of metal hydride formation for the R = Ph case. When both RS^- (R = Me and Et) and MeO^- are present, the higher nucleophilicity of the former anions qualitatively accounts for the preponderance of metal thiolate over metal hydride products.

This postulation is in agreement with our observation that the reaction of **2** with MeSNa *will not proceed in THF*, despite refluxing for 2 h, but went to completion within 15 min at 65 °C upon addition of 1/5 volume of MeOH. We similarly carried out, on an NMR scale, Hidai's reaction of **1**, using MeSNa, and found that in refluxing THF, [(Ind)-$Ru(PPh_3)_2(SMe)$] was the only product, while in refluxing MeOH, the hydride species [(Ind)$Ru(PPh_3)_2H$] was also formed [^{1}H NMR (C_6D_6): δ = –15.39 (t, $^2J_{HP}$ = 33.8 Hz) vs. lit. values in $CDCl_3$: δ = –15.40 (t, $^2J_{HP}$ = 31.6 Hz)[1]]. This indicates that nucleophilic substitution of Cl^- with MeS^- in THF is feasible in **1** but not in **2**, suggestive of the presence of a stronger Ru–Cl bond, which necessitates assistance from MeOH for cleavage. It is likely that **2**, like [$CpRu(PPh_3)_2Cl$] (**1A**), the Cp analogue of **1**, shows appreciable ionic behaviour in MeOH, as shown in Equation (2).

$$[CpRu(PPh_3)_2Cl] + MeOH \rightleftharpoons [CpRu(PPh_3)_2(MeOH)]^+ + Cl^- \quad (2)$$

Indeed, the MeOH complex had been isolated as the BPh_4^- salt,[17] and nucleophilic displacement of chloride in **1A** by nitriles, tertiary phosphanes or phosphites has been shown to proceed by displacement of the weakly bound MeOH.[18] Such a dissociative tendency of the Ru–Cl bond will facilitate the dissociative pathways found to operate in substitution reactions of both Cp and indenyl complexes of Ru.[19] Incidentally, we have noted that the majority of reported reactions of (Ind)Ru complexes have been carried out in MeOH. In this present system, we have also observed, in a small-scale NMR tube reaction, that the solvent derivative of **2**, [(Ind)Ru(dppf)(CH_3CN)]PF_6 (**2S**), reacted with MeSNa in THF at r.t. to give **3** as the sole product. In fact, Stone and co-workers had established that increasing donor ability of phosphane ligands strengthens the Ru–Cl bond sufficiently that displacement of chloride in [$CpRu(L)_2Cl$] (L = phosphane) cannot be effected.[20] Hence the observed stronger Ru–Cl bond in **2** versus its Cp analogue **2A** and versus its bis(PPh_3) analogue **1** [here dppf vs. $(PPh_3)_2$] is in agreement with the recent finding that the indenyl ligand is more electron-donating than Cp towards Ru,[13] as is also confirmed by CV measurements in this study (see cyclic voltammetric and EPR measurements section).

Complex **5** crystallises with one CH_2Cl_2 and 0.5 MeOH in the orthorhombic *Fdd*2 space group, while **6** crystallises in the monoclinic $P2_1/n$ space group. Their molecular structures are very similar to those of their respective Cp analogues,[9b,21] and are illustrated in the ORTEP diagrams shown in Figures 1 and 2. The metal centres are coordinated to η^5-Ind, η^2-dppf and η^1-thiophenolate/hydrido ligands. Selected bond parameters are compared with those of the Cp analogues in Table 1.

The Ru–S distances in **5** and its Cp analogue are comparable and longer than in other examples of Ru–S(thiolate) bonds [2.30 Å (av.)].[23] The Cp rings of dppf in **5** are almost eclipsed (*syn* periplanar) to each other, with a torsional angle (τ) of 2.1°. The phenyl ring on thiophenolate is almost parallel to the phenyl ring on P1, while the phenyl ring of

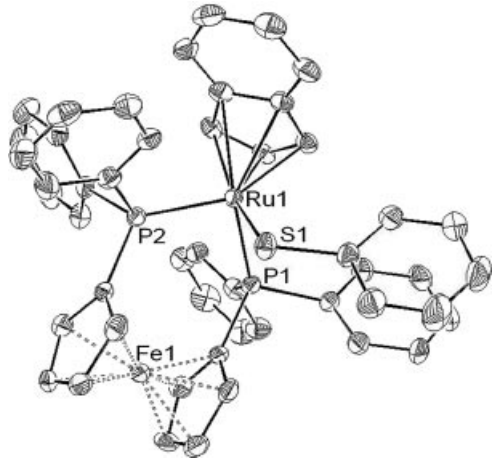

Figure 1. ORTEP diagram of **5**. Thermal ellipsoids are drawn to 50% probability level. Hydrogen atoms are omitted for clarity.

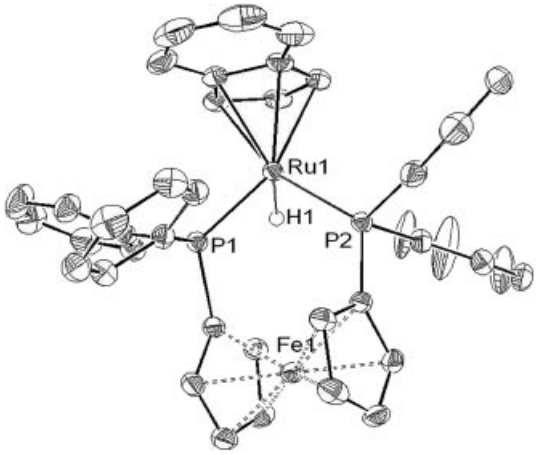

Figure 2. ORTEP diagram of **6**. Thermal ellipsoids are drawn to 50% probability level. Except for the metal hydride atom H1, all other hydrogen atoms are omitted for clarity.

thiophenolate in the Cp analogue points away from the phenyl rings on dppf. This is probably because of the steric bulk of the indenyl ligand, which restricts the orientation of the thiophenolate ligand in **5**.

The hydride ligand in **6** is located in the electron density map and refined with a Ru–H bond length of 1.499(6) Å and P–Ru–H angles of 80.19(2)° and 85.28(2)°. Compared to the eclipsed conformation in **5**, the Cp rings of the dppf in **6** adopt a more stable *syn* clinal (gauche) configuration. This is facilitated because the smaller terminal hydride relieves the steric stress around the Ru centre, enabling the dppf ligand to orientate to the lower-energy *syn* clinal configuration with a torsional angle (τ) of 39.67°. The benzenoid ring of the indenyl ligand was predicted to arrange itself *trans* to the hydride, the higher *trans*-influence ligand,[4d] as shown in Figure 3.

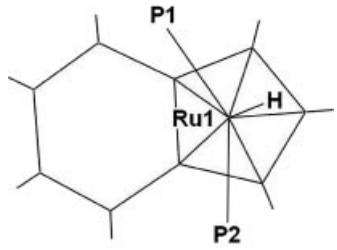

Figure 3. Top view of **6**.

(b) Reaction of 2 with the Mixed-Donor Ligand $^{-}S(CH_2)_2PPh_2$

The reaction in MeOH of **2** with $Ph_2P(CH_2)_2S^-$, a 'hybrid' ligand with two coordinating sites, resulted in a mixture of [(Ind)Ru(η^2-dppf){κ^1*S*-S$(CH_2)_2PPh_2$}] (**7**) and **6** in 54% and 15% yields respectively (Scheme 2), indicating an equilibrium between $Ph_2P(CH_2)_2S^-$ and $Ph_2P(CH_2)_2SH$ in MeOH. This reaction cannot be effected in THF at r.t. or at reflux, as previously observed. The amount of **6** isolated suggested that the pK_a of $Ph_2P(CH_2)_2SH$ is similar to that of EtSH (see Scheme 1).

The ^{1}H NMR and ^{31}P NMR spectra of **7** indicate that the Ru centre is coordinated to η^5-Ind, η^2-dppf and κ^1*S*-2-(diphenylphosphanyl)ethylthiolate [$Ph_2P(CH_2)_2S^-$]; the coordinated phosphorus atoms of dppf resonate at δ = 56.1, while the low-field ^{31}P signal (δ = –14.8 ppm) of the hybrid ligand pertains to a noncoordinating PPh_2 entity, in agreement with the higher nucleophilicity of thiolato sulfur, and hence its better coordinative capability to the Ru^{II} centre when compared to phosphane P. The mixed-donor ligand

Table 1. Selected bond lengths [Å] and angles [°].

Complex	**5**·CH_2Cl_2·0.5MeOH	[CpRu(dppf)(SPh)][9b]	**6**	[CpRu(dppf)H][21]
Δ [Å][22]	0.192	–	0.1205	–
Hinge angle (HA) [°][22]	6.88	–	5.19	–
Fold angle (FA) [°][22]	9.87	–	7.56	–
C*–Ru1[a]	1.939	–	1.923	–
Ru1–P1	2.2523(12)	2.284(3)	2.2446(9)	2.263(4)
Ru1–P2	2.3085(12)	2.302(3)	2.2553(9)	2.246(3)
Ru1–X	X = S1; 2.4193(12)	X = S1; 2.434(4)	X = H; 1.499(6)	X = H; 1.30
P1–Ru1–P2	97.54(4)	99.02(10)	98.68(3)	99.1(1)
P1–Ru1–X	X = S1; 86.21(4)	X = S1; 89.29(11)	X = H; 80.19(2)	–
P2–Ru1–X	X = S1; 86.08(4)	–	X = H; 85.28(2)	–

[a] C* = centroid of the five-membered ring, C1, C2, C3, C3a and C7a.

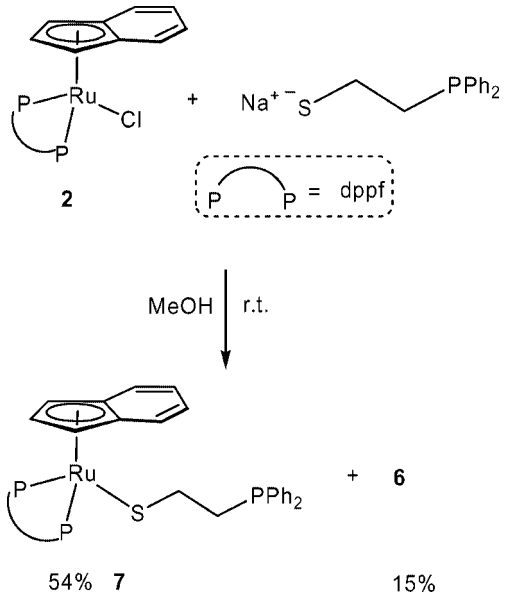

Scheme 2.

displaced neither the indenyl ligand nor dppf, indicating the stronger chelating effect of the dppf ligand versus $Ph_2P(CH_2)_2S^-$.

Cyclic Voltammetric and EPR Measurements

Cyclic voltammograms obtained at a GC electrode in 0.5 mM solutions of **3**, **4**, **5**, **2**, **2A** and **2B** in CH_2Cl_2 at 233 K are shown in Figure 4. On the CV timescale, complexes **3**, **4** and **5** displayed chemically reversible oxidation

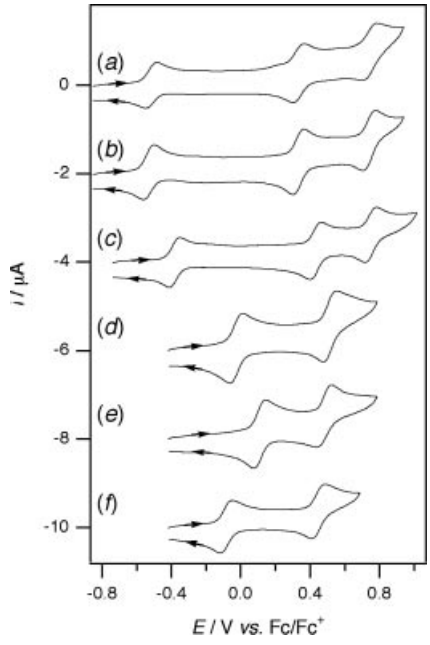

Figure 4. Cyclic voltammograms performed at a 1-mm diameter planar GC electrode in CH_2Cl_2 (0.25 M Bu_4NPF_6) at 233 K at a scan rate of 100 mV s^{-1} for 0.5 mM (a) **3**, (b) **4** (c) **5**, (d) **2**, (e) **2A** and (f) **2B**. CVs in (b), (c), (d), (e) and (f) are offset by –2, –4, –6, –8 and –10 μA respectively.

processes at low temperatures, although at room temperature the third (most-positive) oxidation processes were only partially chemically reversible, suggesting chemical instability of the triply oxidised species. The expression "chemical reversibility", when used in connection with cyclic voltammetry experiments, relates to the ratio of the oxidative (i_p^{ox}) to reductive peak currents (i_p^{red}). The i_p^{ox}/i_p^{red} ratio approaches unity for a fully chemically reversible process.

Complexes **2**, **2A** and **2B** displayed two chemically reversible oxidation processes, except for **2A**, where the second more positive process was only partially chemically reversible at a scan rate of 100 mV s^{-1} (suggesting instability of the more highly oxidised state). At scan rates >100 mV s^{-1}, the i_p^{ox}/i_p^{red} ratio for the second process of **2A** became closer to one. Complexes **3**, **4** and **5** also displayed one chemically irreversible reduction process at about –2.5 V versus Fc/Fc^+ (data not shown), with a similar current magnitude to the first oxidation process (indicating that the same number of electrons were transferred).

Table 2 lists the reversible oxidation potentials ($E^r_{1/2}$) that were calculated from CV data under conditions where the i_p^{ox}/i_p^{red} ratios were equal to unity and using the relationship (3)

$$E^r_{1/2} = (E_p^{ox} + E_p^{red})/2 \quad (3)$$

where E_p^{ox} and E_p^{red} are the anodic and cathodic peak potentials, respectively. In situations where no reverse peak was observed, only the peak potential is given. Voltammetric data from reports on several other related compounds are also given in Table 2. The ΔE values for several of the literature compounds are very large (>>100 mV), indicating complicated electrochemical behaviour, and suggesting that the reported $E^r_{1/2}$ values do not correspond closely to the formal potentials.

In most instances where the E_p^{ox} and E_p^{red} peak separation (ΔE) could be measured, the values obtained were close to that expected for a one-electron transfer (Table 2). There were some variations detected in the peak current intensities for equivalent concentrations of different compounds (Figure 4), but this is likely to be due to differences in diffusion coefficients, as the peak currents appear to approximately inversely correlate with the size of the molecules. Coulometry measurements made during exhaustive controlled potential electrolysis (CPE) experiments at 233 K for the first oxidation process of **3** and **5**, at applied potentials 100 mV more positive than the $E^r_{1/2}$ values, confirmed the transfer of one electron per molecule, see Equation (4) in the Exp. Sect. The one-electron oxidised species were stable for at least 2–3 h at 233 K in CH_2Cl_2 and could be reversibly reduced back to their starting materials. The electrolysis experiments were performed at low temperatures to ensure increased stability of the oxidised compounds (compared to at ambient temperatures).

Free dppf is oxidised at about +200 mV more positive than ferrocene.[24] The product of this one-electron oxidation is not as stable as the Fc/Fc^+ system and moderate scan rates of around 3 V s^{-1} are needed to obtain i_p^{ox}/i_p^{red} ratios equal to unity.[24] When dppf is coordinated to other

Table 2. Cyclic voltammetric data obtained at a scan rate of 100 mV s^{-1} at a 1-mm diameter glassy carbon electrode at 233 K in CH_2Cl_2 with 0.25 M Bu_4NPF_6 as the supporting electrolyte, together with some literature data.

Compound	Oxidation process[a]				Reduction process
	E_p^{ox} [V][b]	E_p^{red} [V][c]	$E^r_{1/2}$ [V][d]	ΔE [mV][e]	E_p^{red} [V][c]
[(η^5-Ind)Ru(PPh_3)$_2$Cl] **1**			–0.01	66[13]	
[(η^5-Ind)Ru(dppf)Cl] **2**	+0.010	–0.062	–0.03	72	not detected
	+0.553	+0.476	+0.51	77	
[(η^5-Ind)Ru(dppf)(SMe)] **3**	–0.480	–0.542	–0.51	62	
	+0.344	+0.288	+0.32	56	
	+0.771	+0.702	+0.74	69	
					–2.620
[(η^5-Ind)Ru(dppf)(SEt)] **4**	–0.498	–0.560	–0.53	62	
	+0.364	+0.300	+0.33	64	
	+0.776	+0.708	+0.74	68	
					–2.610
[(η^5-Ind)Ru(dppf)(SPh)] **5**	–0.351	–0.416	–0.38	65	
	+0.464	+0.399	+0.43	65	
	+0.784	+0.718	+0.75	66	
					–2.548
[(η^5-Ind)Ru(dppe)Cl]			–0.03	64[13]	
[(η^5-Ind)Ru(dppm)Cl]			–0.07	62[13]	
[(η^5-Cp)Ru(dppf)Cl] **2A**	+0.144	0.073	+0.11	71	not detected
	+0.521	+0.436	+0.48	85	
[(η^5-Cp)Ru(dppe)Cl]			+0.05	110[27]	
[(η^5-Cp)Ru(dppm)Cl]			+0.03	340[27]	
[(η^5-Cp)Ru(PPh_3)$_2$Cl] **1A**			+0.10	360[27]	
[(η^5-Cp*)Ru(dppf)Cl] **2B**	–0.050	–0.115	–0.08	65	not detected
	+0.486	+0.408	+0.45	78	
[(η^5-Cp*)Ru(dppe)Cl]			–0.13	270[27]	
[(η^5-Cp*)Ru(PPh_3)$_2$Cl]			–0.03	240[27]	
[(η^5-Ind)Ru(dppf)H] **6**	–0.262	–0.328	–0.30	66	
	–0.072	–0.174	–0.12	102	not detected

[a] All potentials are relative to the Fc/Fc^+ redox couple. Data from literature reports[13,27] that were vs. SCE have been converted to vs. Fc/Fc^+ by adding 0.46 V (corrections for differences in temperature have not been made). [b] E_p^{ox} = oxidative peak potential. [c] E_p^{red} = reductive peak potential. [d] $E^r_{1/2} = (E_p^{ox} + E_p^{red})/2$. [e] $\Delta E = |E_p^{ox} - E_p^{red}|$.

metal ions through the phosphorus atoms, the oxidation potential increases to about +0.5 V versus Fc/Fc^+ and the stability of the oxidised dppf is substantially improved so that i_p^{ox}/i_p^{red} ratios equal to unity are obtained at slow scan rates of 100 mV s^{-1} (similar to Fc/Fc^+).[24,25] In the light of these previous observations,[24,25] we conclude that the oxidation process that occurs at +0.32–0.51 V versus Fc/Fc^+ in the CV's of **3**, **4**, **5**, **2**, **2A** and **2B** (i.e., the second process) is likely to be associated with the one-electron oxidation of [dppf] to $[dppf]^+$. Therefore, the first oxidation process observed in the CV's in Figure 4 is associated with the formal oxidation of Ru^{2+} to Ru^{3+} (although it is likely some electron delocalisation occurs). The conclusion that the first process is associated with localised oxidation of the Ru centre is consistent with a similar first oxidation potential for **3**, **4** and **5** (ca. –0.45 V vs. Fc/Fc^+) and for **2**, **2A** and **2B** (ca. 0 V vs. Fc/Fc^+) (Figure 4), as the potential is likely to be most sensitive to the substituents coordinated directly to the ruthenium. The third oxidation process for **3**, **4** and **5** is possibly again centred on the ruthenium ion, as an Ru^{3+}-to-Ru^{4+} redox transformation is to be expected (although the exact location of the oxidation process is difficult to determine from CV experiments). Complexes **2**, **2A** and **2B** may also be further oxidised, but at a more positive potential than **3**, **4** and **5** (additional oxidation processes were not detected within the solvent/electrolyte potential window).

The $E^r_{1/2}$ values of the complexes (Table 2) indicate ease of oxidation of the complexes as follows: for [LRuCl(dppf)] complexes (L = Ind, Cp and Cp*), Cp* < Ind < Cp, in agreement with the decreasing electron-donor capability of the corresponding ligands. Similar trends have been observed for the dppe, dppm, $(PPh_3)_2$ and $(PMe_2Ph)_2$ analogues.[13,27] The data also show [(Ind)RuCl(dppf)SMe] (**3**) is more easily oxidised than its Ph analogue **5**, in agreement with decrease of electron density at the metal centre in **5**, caused by delocalisation into the Ph ring.

EPR experiments were performed at 10 K on frozen samples of $\mathbf{3}^+$ and $\mathbf{5}^+$ that were produced by electrochemically oxidising the starting materials by one electron at a constant potential at 233 K (Figure 5). The spectrum obtained for $\mathbf{5}^+$ showed additional hyperfine structure, suggesting that the unpaired electron was partially delocalised, possibly on the Ph group bonded to the S. Complex $\mathbf{3}^+$ did not display hyperfine structure, possibly because the unpaired electron was less able to be accommodated about the methyl group bonded to the sulfur. Interaction of the unpaired electron with the ^{31}P atoms (I = ½, 100% abundance) is also possible, as has been observed in diastereomeric [(η^6-arene)Ru^{III}(P-As)Cl] complexes in which the ruthenium atom is a chiral stereocentre.[26] EPR spectra of $\mathbf{3}^+$ or $\mathbf{5}^+$ were not detected at room temperature, indicting that the unpaired electron was mainly localised on the metal ion,

rather than on the organic ligands. The further one-electron oxidation of $\mathbf{3}^+$ and $\mathbf{5}^+$ at 233 K (two electrons overall) produced compounds that did not give an EPR signal at 10 K and above, either because they were diamagnetic or were paramagnetic with rapid relaxation times. Complex $\mathbf{4}^+$ was not examined by EPR spectroscopy because the cyclic voltammetry experiments indicated that its electrochemical behaviour was essentially identical to $\mathbf{3}^+$ (Figure 4).

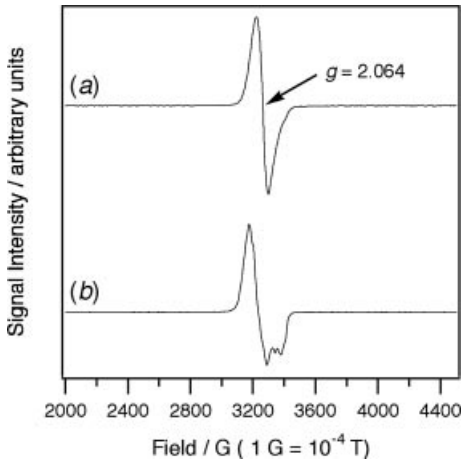

Figure 5. Continuous wave X-band EPR spectra obtained at 10 K with microwave frequency of 9.44 GHz and microwave power of 0.2 mW after the exhaustive electrochemical one-electron oxidation of (a) **3** to $\mathbf{3}^+$ and (b) **5** to $\mathbf{5}^+$ at –0.2 V vs. Fc/Fc^+ in CH_2Cl_2 (with 0.25 M Bu_4NPF_6) at 233 K.

Cyclic voltammograms of [(Ind)Ru(dppf)H] **6** obtained in CH_2Cl_2 solutions at 233 K at a GC electrode are displayed in Figure 6. The compound displayed two chemically reversible (or quasireversible) oxidation processes at about –0.3 and –0.1 V versus Fc/Fc^+. The second oxidation process had smaller peak currents than the first process, which may be caused by interactions between the oxidised compound and the electrode surface. On a Pt electrode, only one drawn out oxidation process was detected between –0.2 and 0.2 V, indicating that the oxidation processes were strongly influenced by the nature of the electrode surface. The cyclic voltammetry significantly changed from that shown in Figure 6 as the temperature was raised,

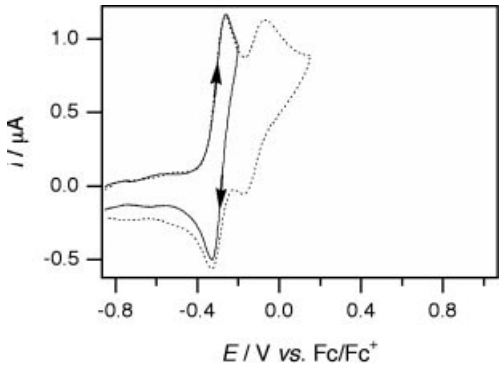

Figure 6. Cyclic voltammograms recorded at 100 $mV s^{-1}$ of a 1.2 mM CH_2Cl_2 solution of **6** with 0.5 M Bu_4NPF_6 at a 1-mm planar GC electrode at 233 K.

because of instability of oxidised **6** in CH_2Cl_2. At 293 K, only one chemically irreversible oxidation process was detected at about +0.6 V versus Fc/Fc^+.

[(Ind)Ru(dppf)H] (**6**) was approximately 0.3 V easier to oxidise than the corresponding Cl complex, [(Ind)Ru(dppf)-Cl] (**2**) (Table 2), which is a similar trend seen for other η^5 organometallic compounds containing the dppf ligand and Cl or H.[28]

Conclusions

Chloro substitution of [(Ind)Ru(dppf)Cl] (**2**) with thiolates (RS^-) in MeOH was found to yield both thiolato derivatives and a hydrido complex, [(Ind)Ru(dppf)H] (**6**), the yield of which is both solvent- and R-dependent. From observations that the reaction could not proceed in the absence of MeOH, it was rationalised that **6** was formed by β-H elimination from ligated MeO^-, the latter being formed in equilibrium amounts by an interaction between RS^- and MeOH. The product mixture therefore reflected the relative nucleophilicity of RS^- and MeO^-. Voltammetry experiments indicated that the formal oxidation potentials for [LRu(dppf)Cl] compounds (L = Ind, Cp and Cp*) occurred in the order Cp* < Ind < Cp, with a 200 mV difference between the Cp* and Cp compounds. For [(Ind)Ru(L′)Cl] compounds {L′ = dppm, dppe, dppf, $(PPh_3)_2$}, the formal potentials decreased in the order dppm < dppe/dppf < $(PPh_3)_2$, although the total difference in oxidation potential spanning all the different diphosphanes [(Ind)Ru(L′)Cl] was a relatively small 60 mV. EPR experiments on $\mathbf{3}^+$ and $\mathbf{5}^+$ at 10 K indicated that the monocations were paramagnetic and the dications were EPR silent.

Experimental Section

General: All reactions were carried out using conventional Schlenk techniques under inert nitrogen or argon in an M. Braun Labmaster 130 Inert Gas System.

NMR spectra were measured with a Bruker 300 FT NMR spectrometer; for ^1H and ^{31}P spectra, chemical shifts were referenced to residual solvent in the deuterio-solvents. IR spectra in KBr pellets were measured in the range 4000–400 cm^{-1} by means of a BioRad FTS-165 FTIR instrument. Mass spectra were run on a Finnigan Mat 95XL-T (FAB) or a Finnigan-MAT LCQ (ESI) spectrometer. Elemental analyses were performed by the microanalytical laboratory in-house.

[(Ind)Ru(PPh_3)$_2$Cl] (**1**)[1] and $Ph_2P(CH_2)_2SH$[29] were prepared by published methods. [(Ind)Ru(dppf)Cl] (**2**) was synthesised from phosphane substitution of **1**, while [(Ind)Ru(dppf)(CH_3CN)]PF_6 (**2S**) was derived from **2** by reaction with $NaPF_6$ in refluxing CH_3CN.[30] All other chemicals were obtained commercially and used without any further purification. All solvents were dried with sodium/benzophenone and distilled before use. Celite (Fluka AG) and silica gel (Merck Kieselgel 60, 230–400 mesh) were dried at 140 °C overnight before chromatographic use.

Electrochemical Studies: Voltammetric experiments were conducted with a computer-controlled Eco Chemie µAutolab III potentiostat. Solutions of electrogenerated compounds for the EPR experiments

were prepared in a divided controlled potential electrolysis cell separated with a porosity no. 5 (1.0–1.7 μm) sintered glass frit. The working and auxiliary electrodes were identically sized Pt mesh plates symmetrically arranged with respect to each other. A silver wire reference electrode (isolated by a salt bridge containing 0.5 M Bu_4NPF_6 in CH_3CN) was positioned to within 2 mm of the surface of the working electrode. The electrolysis cell was jacketed in a glass sleeve and cooled to 233 K (for improved stability of the oxidised compounds) using a Lauda RL6 variable temperature methanol-circulating bath. The volumes of both the working and auxiliary electrode compartments were approximately 20 mL each. The number of electrons transferred during the bulk oxidation process was calculated from Equation (4)

$$N = Q/nF \quad (4)$$

where N is the number of mols of the starting compound, Q is the charge (coulombs), n is the number of electrons and F is the Faraday constant (96485 C mol^{-1}). The electrolysed solutions were transferred under vacuum into cylindrical 3-mm (id) EPR tubes that were immediately frozen in liquid N_2. EPR spectra were recorded with a Bruker ESP 300e spectrometer in a TE_{102} cavity at 10 K using liquid He cooling.

Synthesis of [(Ind)Ru(dppf)(SR)] {R = Me (3), Et (4), Ph (5)}: RSNa {0.25 mmol: R = Me, 17 mg; R = Et [freshly prepared in situ from EtSH (19 μL) and MeONa obtained from 6 mg Na in 2 mL MeOH]; R = Ph, 33 mg} was added to a red suspension of [(Ind)-Ru(dppf)Cl] (**2**) (50 mg, 0.062 mmol) in MeOH (5 mL) and the mixture was stirred, whereupon the colour of the suspension changed immediately to green. After stirring at r.t. for 18 h, the solvent was removed in vacuo and the residue was extracted using toluene (2 × 5 mL). The extract was concentrated to about 2 mL and then loaded onto a silica gel column (2 × 5 cm) prepared in *n*-hexane. Elution gave two fractions: (i) a yellow eluate in toluene (about 8 mL), which yielded [(Ind)Ru(dppf)H] (**6**) (for the reaction in which R = Me, 9 mg, 19% yield; R = Et, 8 mg, 16% yield); (ii) a green eluate in toluene/THF (20:1, about 10 mL), which yielded [(Ind)Ru(dppf)(SR)] {R = Me (**3**), 40 mg, 79% yield; R = Et (**4**), 33.5 mg, 65% yield; R = Ph (**5**), 52 mg, 96% yield}; (iii) an orange-red eluate in THF (3 mL), which gave **2** in trace amounts.

Compound **3** was also formed from the reaction of [(Ind)-Ru(dppf)(CH_3CN)]PF_6 (**2S**) with MeSNa as follows: MeSNa (2 mg, 0.029 mmol) was added to a yellow solution of **2S** (5 mg, 0.005 mmol) in THF (2 mL) and the mixture was stirred at r.t. The colour of the mixture slowly changed from yellow to green in 4 h. The ^{1}H and ^{31}P NMR spectra of an aliquot of the product mixture showed the sole presence of **3**.

Data for 3: ^{1}H NMR (C_6D_6): δ = 1.96 (s, 3 H, SMe), 3.36, 3.89, 3.92 and 4.06 (each s, 2 H, C_5H_4), 5.29 (s, 1 H, Ind), 5.60 (s, 2 H, Ind), 7.04–7.58 (m, 24 H, Ind and Ph) ppm. ^{31}P{^{1}H} NMR (C_6D_6): δ = 56.0 (s, dppf) ppm. FAB$^+$-MS: *m*/*z* (%) = 818 [M]$^+$, 771 [M – SMe]$^+$, 655 [M – SMe – Ind]$^+$. $C_{44}H_{38}FeP_2RuS$ (817.70): calcd. C 64.6, H 4.7, S 3.9; found C 64.7, H 4.8, S 3.9.

(*Note:* The proton resonances of the five-membered ring of Ind in this complex, as in others in this work, appear as singlets, although couplings are anticipated, most probably because these are too small to be resolved using the 300-MHz instrument.)

Data for 4: ^{1}H NMR (C_6D_6): δ = 1.62 (t, $^3J_{HH}$ = 7.4 Hz, 3 H, SCH_2CH_3), 2.16 (q, $^3J_{HH}$ = 7.4 Hz, 2 H, SCH_2CH_3), 3.63, 3.89, 3.94 and 4.06 (each s, 2 H, C_5H_4), 5.27 (s, 1 H, Ind), 5.70 (s, 2 H, Ind), 7.04–7.57 (m, 24 H, Ind and Ph) ppm. ^{31}P{^{1}H} NMR (C_6D_6): δ = 56.1 (s, dppf) ppm. FAB$^+$-MS: *m*/*z* (%) = 832 [M]$^+$, 771 [M – SEt]$^+$, 655 [M – SEt – Ind]$^+$. $C_{45}H_{40}FeP_2RuS$ (831.73): calcd. C 65.0, H 4.9, S 3.9; found C 65.5, H 5.1, S 3.4.

Data for 5: ^{1}H NMR (C_6D_6): δ = 3.62, 3.79, 3.88 and 4.06 (each s, 2 H, C_5H_4), 5.25 (s, 1 H, Ind), 5.64 (s, 2 H, Ind), 6.38–6.40, 6.94–6.97 (each 4-line m, 2 H, Ind), 7.04–7.58 (m, 20 H, Ph) ppm. ^{31}P{^{1}H} NMR (C_6D_6): δ = 54.9 (s, dppf) ppm. FAB$^+$-MS: *m*/*z* (%) = 880 [M]$^+$, 771 [M – SPh]$^+$, 655 [M – SPh–Ind]$^+$. $C_{49}H_{40}FeP_2RuS$ (879.77): calcd. C 66.9, H 4.6, S 3.6; found C 67.3, H 4.8, S 4.1.

Small-Scale Reactions of 1 with MeSNa in MeOH and THF – Effect of Solvent: MeSNa (2 mg, 0.029 mmol) was added to a red solution or suspension of **1** (5 mg, 0.006 mmol) in the selected solvent (1 mL), and the mixture was refluxed. After the reaction, the product mixture was evacuated to dryness and the respective residues extracted with toluene, for examination by ^{1}H and ^{31}P NMR spectroscopy.

(i) In MeOH: A reflux for 1 h produced a suspension of dark green solids in a faint yellow supernatant. The spectra indicated the product was a mixture of [(Ind)Ru(PPh_3)$_2$(SMe)] (**3P**) and the hydride species [(Ind)Ru(PPh_3)$_2$H] [^{1}H NMR (C_6D_6): δ = –15.39 ppm (t, $^2J_{HP}$ = 33.8 Hz), cf. lit. values in $CDCl_3$: δ = –15.40 ppm (t, $^2J_{HP}$ = 31.6 Hz)[1]] in the ratio of 1:1.

(ii) In THF: The solution changed slowly to dark green during reflux (2 h). The spectra indicated that [(Ind)Ru(PPh_3)$_2$(SMe)] (**3P**) was the sole product.

Data for 3P: ^{1}H NMR (C_6D_6): δ = 2.23 (s, 3 H, SMe), 4.30 (s, 2 H, Ind), 5.22 (s, 1 H, Ind), 6.88–7.47 (m, 34 H, Ind and Ph) ppm. ^{31}P{^{1}H} NMR (C_6D_6): δ = 50.2 (s, PPh_3) ppm.

Reaction of 2 with MeONa (in THF/MeOH): Complex **2** (10 mg, 0.012 mmol) as a red solid was added to a suspension of dry MeONa [freshly prepared from Na (6 mg, 0.26 mmol) in MeOH (4 mL)] in THF (5 mL), and the slurry stirred at r.t. The ^{1}H and ^{31}P NMR spectra in C_6D_6 of aliquots of the reaction mixture at 2 h, and after reflux for an additional 4 h, revealed that the reaction did not proceed. MeOH (1 mL) was then added into the mixture and stirring continued at r.t. A slow colour change from orange-red to yellow occurred within 1 h. The ^{1}H and ^{31}P NMR spectra of an aliquot in C_6D_6 showed the formation of **6** as the sole product.

Data for 6: ^{1}H NMR (C_6D_6): δ = –15.4 (t, $^2J_{HP}$ = 33 Hz, 1 H), 3.77 (s, 4 H, C_5H_4), 4.13 and 4.27 (each s, 2 H, C_5H_4), 4.34 (s, 2 H, Ind), 5.75 (s, 1 H, Ind), 6.28–6.31, 6.80–6.83 (each 4-line m, 2 H, Ind), 7.12–7.19, 7.28–7.33 and 8.03–8.08 (each m, total 20 H, Ph) ppm. ^{31}P{^{1}H} NMR (C_6D_6): δ = 62.9 (s, dppf) ppm. ESI$^+$-MS: *m*/*z* (%) = 772 [M + H]$^+$. $C_{43}H_{36}FeP_2Ru$ (771.61): calcd. C 66.9, H 4.7; found C 66.9, H 4.5.

Synthesis of [(Ind)Ru(dppf){S(CH_2)$_2$$PPh_2$}] (7): $Ph_2P(CH_2)_2SH$ (54 μL, 0.25 mmol) was added into excess NaH in THF (5 mL) and the suspension was stirred at r.t. overnight. The suspension was filtered through Celite into a red suspension of **2** (50 mg, 0.06 mmol) in MeOH (10 mL). The reaction mixture was stirred at r.t. for 18 h. A slow colour change from red suspension to dark green solution was observed. The solvent was removed in vacuo, and the residue extracted with toluene (2 × 5 mL). The toluene extract was concentrated to about 1 mL and loaded onto a silica gel column (2 × 10 cm) prepared in *n*-hexane. Elution gave two fractions: (i) a yellow eluate in toluene (about 4 mL), which gave **6** (7 mg, 15% yield); and (ii) a dark green eluate in toluene/diethyl ether (1:1, about 10 mL), which yielded [(Ind)Ru(dppf){S(CH_2)$_2$-PPh_2}] (**7**) (34 mg, 54% yield).

Data for 7: ^{1}H NMR (C_6D_6): δ = 2.31–2.39 and 2.75–2.80 (each m, 2 H, CH_2), 3.64, 3.88, 3.92 and 4.06 (each s, 2 H, C_5H_4), 5.18

Table 3. Crystal and structure refinement data.

	5·CH_2Cl_2·0.5MeOH	**6**
Formula	$C_{50.50}H_{44}Cl_2FeO_{0.50}P_2RuS$	$C_{43}H_{36}FeP_2Ru$
Formula mass	980.68	771.58
Space group (crystal system)	*Fdd*2	$P2_1/n$
Crystal system	orthorhombic	monoclinic
Unit cell dimensions		
a [Å]	27.452(3)	11.8603(7)
b [Å]	56.029(7)	15.3521(10)
c [Å]	11.6643(14)	18.9672(12)
α [°]	90	90
β [°]	90	98.300(2)
γ [°]	90	90
Cell volume [Å^3]	17941(4)	3417.4(4)
Z	16	4
$D_{calcd.}$ [g cm^{-3}]	1.452	1.500
Absorption coefficient [mm^{-1}]	0.933	0.991
F(000) electrons	8016	1576
Crystal size [mm]	0.36 × 0.12 × 0.10	0.26 × 0.14 × 0.06
θ range for data collection [°]	2.08–26.37	2.17–26.37
Index ranges	$0 \le h \le 34$, $0 \le k \le 70$, $-14 \le l \le 14$	$-14 \le h \le 14$, $0 \le k \le 19$, $0 \le l \le 23$
Reflections collected	60968	27911
Independent reflections	9164	6985
Max. and min. transmission	0.9125–0.7300	0.9429–0.7827
Data/restraints/parameters	9164/3/520	6985/0/428
Gof	1.203	1.053
Final *R* indices [$I > 2\sigma(I)$]	R_1 = 0.0440, wR_2 = 0.1091	R_1 = 0.0465, wR_2 = 0.0927
R indices (all data)	R_1 = 0.0462, wR_2 = 0.1102	R_1 = 0.0640, wR_2 = 0.0994
Largest diff. peak and hole [e Å^{-3}]	0.954 and –0.522	0.618 and –0.443

(s, 1 H, Ind), 5.67 (s, 2 H, Ind), 7.03–7.05 (m, 8 H, Ph), 7.42 (br. s, 5 H, Ph), 7.56–7.61 (m, 7 H, Ph) ppm. $^{31}P\{^1H\}$ NMR (C_6D_6): δ = –14.8 [s, $S(CH_2)_2PPh_2$], 56.1 (s, dppf) ppm. FAB$^+$-MS: *m*/*z* (%) = 1016 [M]$^+$, 771 [M – $S(CH_2)_2PPh_2$]$^+$. $C_{57}H_{49}FeP_3RuS$ (1015.90): calcd. C 67.4, H 4.9, S 3.2; found C 67.7, H 5.0, S 3.2.

Crystal Structure Determinations: Crystals were mounted on quartz fibres. X-ray data were collected on a Bruker AXS APEX system, using Mo-K_α radiation, with the SMART suite of programs.[31] Data were processed and corrected for Lorentz and polarisation effects with SAINT,[32] and for absorption effects with SADABS.[33] Structural solution and refinement were carried out with the SHELXTL suite of programs.[34] Crystal and structure refinement data are summarised in Table 3. The structures were solved by direct methods or Patterson maps to locate the heavy atoms, followed by difference maps for the light, non-hydrogen atoms. All non-hydrogen atoms were generally given anisotropic displacement parameters in the final model.

Two solvent molecules were found for **5**: a dichloromethane and a half-molecule of methanol. The latter was refined with a common isotropic thermal parameter each for the O and C atoms, and the C–O bond length was restrained at 1.45(2) Å.

CCDC-621607 (for **5**·CH_2Cl_2·0.5MeOH) and -621608 (for **6**) contain the supplementary crystallographic data for this paper. These data can be obtained free of charge from The Cambridge Crystallographic Data Centre via www.ccdc.cam.ac.uk/data_request/cif.

Acknowledgments

Support from the National University of Singapore under Academic Research Fund grant No. R-143-000-209-112 to L. Y. G. and a research scholarship to S. Y. N. from the Institute of Chemical and Engineering Sciences (ICES) are gratefully acknowledged. R. D. W. thanks the Australian National University for financial support.

[1] L. A. Oro, M. A. Ciriano, M. Campo, C. Foces-Foces, F. H. Cano, *J. Organomet. Chem.* **1985**, *289*, 117.
[2] a) O. A. Gansow, A. R. Burke, W. D. Vernon, *J. Am. Chem. Soc.* **1976**, *98*, 5817; b) A. Eisenstadt, F. Frolow, A. Efraty, *J. Chem. Soc., Chem. Commun.* **1982**, 642.
[3] P. Alvarez, J. Gimeno, E. Lastra, S. García-Granda, J. F. Van der Maelen, M. Bassetti, *Organometallics* **2001**, *20*, 3762.
[4] a) J. M. O'Connor, C. P. Casey, *Chem. Rev.* **1987**, *87*, 307; b) M. E. Rerek, L. N. Ji, F. Basolo, *J. Chem. Soc., Chem. Commun.* **1983**, 1208; c) V. Cadierno, J. Díez, M. P. Gamasa, J. Gimeno, E. Latra, *Coord. Chem. Rev.* **1999**, *193–195*, 147; d) J. W. Faller, R. H. Crabtree, A. Habib, *Organometallics* **1985**, *4*, 929; e) R. T. Baker, T. H. Tulip, *Organometallics* **1986**, *5*, 839.
[5] See the following and references cited therein: a) J. Díez, M. P. Gamasa, J. Gimeno, E. Lastra, A. Villar, *Organometallics* **2005**, *24*, 1410; b) S. Conejero, J. Díez, M. P. Gamasa, J. Gimeno, *Organometallics* **2004**, *23*, 6299; c) M. Bassetti, P. Alvarez, J. Gimeno, E. Lastra, *Organometallics* **2004**, *23*, 5127; d) P. Alvarez, E. Lastra, J. Gimeno, M. Bassetti, L. R. Falvello, *J. Am. Chem. Soc.* **2003**, *125*, 2386; e) V. Cadierno, M. P. Gamasa, J. Gimeno, C. González-Bernardo, E. Pérez-Carreño, S. García-Granda, *Organometallics* **2001**, *20*, 5177; f) M. P. Gamasa, J. Gimeno, B. M. Martín-Vaca, J. Borge, S. García-Granda, E. Pérez-Carreño, *Organometallics* **1994**, *13*, 4045.
[6] See leading references in: a) ref.[5f]; b) ref.[13]; c) A. Ceccon, S. Santi, L. Orian, A. Bisello, *Coord. Chem. Rev.* **2004**, *248*, 683.
[7] a) K. M. Rao, E. K. Rymmai, *Polyhedron* **2003**, *22*, 307; b) S. S. Keisham, Y. A. Mozharivskyj, P. J. Carroll, M. R. Kollipara, *J. Organomet. Chem.* **2004**, *689*, 1249; c) K. S. Singh, G. P. A. Yap, K. A. Kreisel, M. R. Kollipara, *J. Coord. Chem.* **2005**, *58*, 1607; d) P. Govindaswamy, C. Sinha, M. R. Kollipara, *J. Organomet. Chem.* **2005**, *690*, 3465; e) K. S. Singh, Y. A. Mozharivskyj, C. Thöne, M. R. Kollipara, *J. Organomet. Chem.* **2005**, *690*, 3720; f) K. S. Singh, C. Thöne, M. R. Kollipara, *J. Or-*

ganomet. Chem. **2005**, *690*, 4222; g) K. S. Singh, C. Thöne, M. R. Kollipara, *J. Coord. Chem.* **2006**, *59*, 333.
[8] T. Sato, M. Nishio, Y. Ishii, H. Yamazaki, M. Hidai, *J. Organomet. Chem.* **1998**, *569*, 98.
[9] a) X. L. Lu, J. J. Vittal, E. R. T. Tiekink, G. K. Tan, S. L. Kuan, L. Y. Goh, T. S. A. Hor, *J. Organomet. Chem.* **2004**, *689*, 1978; b) X. L. Lu, J. J. Vittal, E. R. T. Tiekink, L. Y. Goh, T. S. A. Hor, *J. Organomet. Chem.* **2004**, *689*, 1444.
[10] A. Shaver, P. V. Plouffe, P. Bird, E. Livingstone, *Inorg. Chem.* **1990**, *29*, 1826.
[11] M. P. Gamasa, J. Gimeno, C. Gonzalez-Bernardo, B. M. Martín-Vaca, J. Borge, S. Garcia-Granda, *Inorg. Chim. Acta* **2003**, *347*, 181.
[12] a) J. Chatt, B. L. Shaw, *Chem. Ind. (London)* **1960**, 931; b) J. Chatt, B. L. Shaw, *J. Chem. Soc.* **1962**, 5075 and references cited therein.
[13] a) M. I. Bruce, M. G. Humphrey, A. G. Swincer, R. C. Wallis, *Aust. J. Chem.* **1984**, *37*, 1747; b) T. Wilczewski, M. Bocheńska, J. F. Biernat, *J. Organomet. Chem.* **1981**, *215*, 87.
[14] Estimated from observed trends of $\Delta(pK_{a(MeOH)} - pK_{a(water)}) \approx 4.0$ for RSH and the known pK_a value (10.3) of MeSH, in water. [See: E. P. Serjeant, B. Dempsey (Eds.), *Inoization Constants of Organic Acids in Solution, IUPAC Chemical Data Series No. 23*, Pergamon Press, Oxford, UK, **1979**.]
[15] J. F. Bunnett, L. A. Retallick, *J. Am. Chem. Soc.* **1967**, *89*, 423.
[16] B. W. Clare, D. Cook, E. C. F. Ko, Y. C. Mac, A. J. Parker, *J. Am. Chem. Soc.* **1966**, *88*, 1911 and references cited therein.
[17] R. J. Haines, A. L. Du Preez, *J. Organomet. Chem.* **1975**, *84*, 357.
[18] G. S. Ashby, M. I. Bruce, I. B. Tomkins, R. C. Wallis, *Aust. J. Chem.* **1979**, *32*, 1003.
[19] M. P. Gamasa, J. Gimeno, C. Gonzalez-Bernardo, B. M. Martín-Vaca, D. Monti, M. Bassetti, *Organometallics* **1996**, *15*, 302.
[20] T. Blackmore, M. I. Bruce, F. G. A. Stone, *J. Chem. Soc. A* **1971**, 2376.
[21] M. I. Bruce, I. R. Butler, W. R. Cullen, G. A. Koutsantonis, M. R. Snow, E. R. T. Tiekink, *Aust. J. Chem.* **1988**, *41*, 963.
[22] A. K. Kakkar, N. J. Taylor, T. B. Marder, J. K. Shen, N. Hallinan, F. Basolo, *Inorg. Chim. Acta* **1992**, *198–200*, 219.
[23] a) A. Shaver, P. V. Plouffe, D. C. Liles, E. Singleton, *Inorg. Chem.* **1992**, *31*, 997; b) R. Y. C. Shin, M. A. Bennett, L. Y. Goh, W. Chen, D. C. R. Hockless, W. K. Leong, K. Mashima, A. C. Willis, *Inorg. Chem.* **2003**, *42*, 96.
[24] B. Corain, B. Longato, G. Favero, D. Ajo, G. Pilloni, U. Russo, F. R. Kreissl, *Inorg. Chim. Acta* **1989**, *157*, 259.
[25] A. C. Ohs, A. L. Rheingold, M. J. Shaw, C. Nataro, *Organometallics* **2004**, *23*, 4655.
[26] P. A. Gugger, A. C. Willis, S. B. Wild, G. A. Heath, R. D. Webster, J. H. Nelson, *J. Organomet. Chem.* **2002**, *643–644*, 136.
[27] P. M. Treichel, D. A. Khomar, P. J. Vincenti, *Synth. React. Inorg. Met.-Org. Chem.* **1984**, *14*, 383.
[28] R. T. Hembre, J. S. McQueen, V. W. Day, *J. Am. Chem. Soc.* **1996**, *118*, 798.
[29] J. Chatt, J. R. Dilworth, J. A. Schmutz, J. A. Zubieta, *J. Chem. Soc., Dalton Trans.* **1979**, 1595.
[30] S. Y. Ng, G. Fang, W. K. Leong, L. Y. Goh, M. V. Garland, *Eur. J. Inorg. Chem.* **2007**, 452–462.
[31] *SMART* version 5.628, Bruker AXS Inc., Madison, WI, USA, **2001**
[32] *SAINT+* version 6.22a, Bruker AXS Inc., Madison, WI, USA, **2001**
[33] G. M. Sheldrick, *SADABS*, University of Göttingen, Germany, **1996**
[34] *SHELXTL* version 5.1, Bruker AXS Inc., Madison, WI, USA, **1997**

Received: September 20, 2006
Published Online: November 27, 2006

